

# Modeling Geometric Nonlinearities in the Free Vibration of a Planar Beam Flexure With a Tip Mass

**Hamid Moeenfarid**

Department of Engineering,  
School of Mechanical Engineering,  
Ferdowsi University of Mashhad,  
Vakil Abad Boulevard,  
Mashhad, Khorasan Razavi 9177948974, Iran  
e-mail: h\_moeenfarid@um.ac.ir

**Shorya Awtar**

Department of Mechanical Engineering,  
University of Michigan,  
2350 Hayward Street,  
Ann Arbor, MI 48109  
e-mail: awtar@umich.edu

*The objective of this work is to analytically study the nonlinear dynamics of beam flexures with a tip mass undergoing large deflections. Hamilton's principle is utilized to derive the equations governing the nonlinear vibrations of the cantilever beam and the associated boundary conditions. Then, using a single mode approximation, these nonlinear partial differential equations are reduced to two coupled nonlinear ordinary differential equations. These equations are solved analytically using the multiple time scales perturbation technique. Parametric analytical expressions are presented for the time domain response of the beam around and far from its internal resonance state. These analytical results are compared with numerical ones to validate the accuracy of the proposed analytical model. Compared with numerical solution methods, the proposed analytical technique shortens the computational time, offers design insights, and provides a broader framework for modeling more complex flexure mechanisms. The qualitative and quantitative knowledge resulting from this effort is expected to enable the analysis, optimization, and synthesis of flexure mechanisms for improved dynamic performance. [DOI: 10.1115/1.4026147]*

## 1 Introduction and Motivation

Beam flexures are one of the most important building blocks in flexure mechanisms. Flexure mechanisms provide guided motion via elastic deformation, instead of employing sliding or rolling joints, and are used in a variety of applications that demand high precision, minimal assembly, long operating life, or design simplicity [1,2]. Since they exhibit motion guidance as well as elastic behavior, flexure mechanisms are also well-suited for applications, such as single-axis and multi-axis resonators, energy harvesting devices, and high-speed scanners, where dynamics is important.

Large motion range in flexure mechanisms implies large elastic deflections of the constituent beams, which in turn give rise to geometric nonlinearities [1,3]. Even though sometimes ignored, these nonlinearities critically influence the dynamic characteristics of beams [4]. In a flexure mechanism, the elastic motion provided via flexure beams is transferred to one or more moving stages. For example, consider the parallel-kinematic flexure mechanism

shown in Fig. 1, comprising a complex but systematic arrangement of beam flexures and rigid stages [5]. This flexure mechanism provides large and decoupled  $X$  and  $Y$  displacements at the motion stage, with small cross-axis and parasitic errors, and good actuator isolation. This design and its variations are being developed for desktop-scale nanopositioning [6], MEMS scanning [7], and multi-axis energy harvesting applications, all of which are critically affected by the dynamics of the flexure mechanism. Moreover, given the range of flexure displacement, linear analysis proves to be inadequate in capturing the experimentally observed dynamic characteristics [6]. Depending on the application, the relevant dynamic characteristics include vibrational mode-shapes, flow of energy between modes, bandwidth or speed of response, command tracking, noise and disturbance sensitivity, closed-loop stability, and robustness, etc.

As a result, it is crucial that the flexure mechanism is designed and optimized for dynamic performance in a given application. A logical first step in a broader study of the dynamics of flexure mechanisms is to consider and understand the dynamics of a simple beam with a tip mass in terms of its end point displacements. Such a study is the focus of this paper. This helps elucidate what nonlinearities influence the dynamic behavior, what kind of dynamic behavior is seen as a consequence, and how the flexure beam physical parameters (i.e., geometry, material, etc.) can be selected to mitigate or accentuate certain dynamic behavior.

In general, nonlinearities may arise from the geometry of deformation or from material properties. Geometric nonlinearity arises from arc-length conservation of the beam and large deformation curvatures due to which the linear relationship between displacement field and strains no longer holds. Material nonlinearity occurs when the stresses are nonlinear functions of strains [8].

Because of its long, slender geometry, a uniform-thickness planar beam flexure may be modeled using the Euler-Bernoulli beam theory. This theory assumes that plane cross-sections continue to remain plane and normal to the neutral axis after deformation [9] and has been successfully utilized to study the static, dynamic, and vibrational behavior of beams. In particular, large-amplitude vibrations of beams have been extensively investigated both theoretically and experimentally in the literature. Crespo da Silva [10] formulated the nonlinear differential equations of motion for Euler-Bernoulli beams experiencing flexure along two principle directions, along with torsion and extension. Furthermore, Crespo da Silva [11] presented a reduced-order analytical model for the nonlinear dynamics of a class of flexible multi-beam structures. Nayfeh [12] modeled the nonlinear transverse vibration of beams with properties that vary along the length. Zaretzky and da Silva [13] experimentally investigated the nonlinear modal coupling in the response of cantilever beams.

The presence of a tip mass on the beam changes the differential equations governing its deflection. This is because the inertial force exerted on the beam due to the presence of a concentrated mass is a function of the deflection itself. Large-amplitude vibrations of beams with tip mass have also been investigated in the literature. Hijmissen and Horssen [14] analyzed the weakly damped transverse vibrations of a vertical beam with a tip mass. Zavodney and Nayfeh [15] studied the nonlinear response of a slender beam carrying a lumped mass to a principle parametric excitation. But the axial dynamics of the beam, which can become important at large deflections, was not considered in these formulations. The dynamics of beam-based flexure mechanisms has also been investigated using the pseudorigid body modeling method [16]. While this method simplifies the large deflection nonlinear analysis of flexure mechanisms by modeling them as lumped-parameter rigid-body mechanisms, it does not capture the effects of axial stretching in individual beams.

This paper presents an analytical investigation of the nonlinear in-plane oscillations of a flexure beam with a tip mass, while including axial stretching. With this problem definition, the partial differential equations governing the dynamics of this system are

Contributed by the Mechanisms and Robotics Committee of ASME for publication in the JOURNAL OF MECHANICAL DESIGN. Manuscript received August 27, 2012; final manuscript received November 27, 2013; published online February 26, 2014. Assoc. Editor: Craig Lusk.

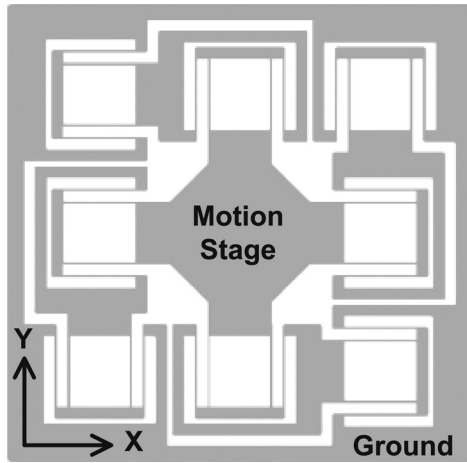


Fig. 1 A parallel-kinematic XY flexure mechanism [5]

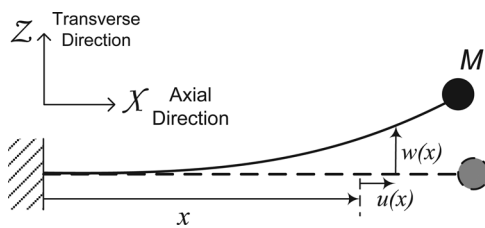


Fig. 2 Schematic view of a beam with a tip mass

derived. Using a single mode approximation, these equations are reduced to coupled, ordinary, nonlinear differential equations. Using a physically justified scaling of the problem's variables, these equations are solved using the perturbation method of multiple time scales [8].

The specific contributions of this paper are (1) a first-time investigation of the planar dynamics (transverse bending and axial stretching) of a flexure beam with a tip mass while including geometric nonlinearities. (2) A new analytical solution of these equations, albeit using known derivation and solution techniques, which relates the beam's design parameters to its dynamic behavior. (3) Design insights into which geometric nonlinearities affect the beam dynamics and how the dimensions and material of the beam can be chosen to mitigate or accentuate certain dynamic behavior.

## 2 Problem Formulation

The beam with tip-mass considered in this analysis is shown in Fig. 2. The dashed line represents the undeformed state, while the solid line represents a general deformed state. The gravitational field, if any, is assumed normal to the plane and therefore does not affect the planar analysis considered here.

As the first step, the equations of motion and boundary conditions corresponding to the transverse and axial vibrations of a slender beam will be derived using the generalized Hamilton's principle. In the Euler-Bernoulli beam theory, plane cross-sections remain plane and perpendicular to the neutral axis after deformation, which implies that distortions due to shear are neglected. These assumptions are applicable for long and slender beams, with length much greater than the thickness [9]. Since the beam undergoes large deflections, the nonlinear strain expression is used for calculating its strain energy.

The axial strain at a differential element at distance  $z$ , along the  $Z$  direction, from the neutral axis may be expressed as follows [17]:

$$\epsilon_{xx} = \frac{\partial u}{\partial x} + \frac{1}{2} \left( \frac{\partial w}{\partial x} \right)^2 - z \left( \frac{\partial^2 w}{\partial x^2} \right) \quad (1)$$

where  $u$  and  $w$  are the displacements along  $X$  and  $Z$  axes, respectively.

Using Eq. (1), the strain energy of the beam assuming linear elastic material properties would be

$$\begin{aligned} \pi &= \frac{E}{2} \iint \int_V \epsilon_{xx}^2 dA \cdot dx = \frac{E}{2} \iint \int_0^l \left[ \left( \frac{\partial u}{\partial x} + \frac{1}{2} \left( \frac{\partial w}{\partial x} \right)^2 \right)^2 \right. \\ &\quad \left. + \left( \frac{\partial^2 w}{\partial x^2} \right)^2 z^2 - 2z \frac{\partial^2 w}{\partial x^2} \left( \frac{\partial u}{\partial x} + \frac{1}{2} \left( \frac{\partial w}{\partial x} \right)^2 \right) \right] dA \cdot dx \\ &= \frac{1}{2} \int_0^l E \cdot A(x) \left( \frac{\partial u}{\partial x} + \frac{1}{2} \left( \frac{\partial w}{\partial x} \right)^2 \right)^2 dx + \frac{1}{2} \int_0^l E \cdot I(x) \left( \frac{\partial^2 w}{\partial x^2} \right)^2 dx \end{aligned} \quad (2)$$

where  $l$  is the undeformed length of the beam,  $A(x)$  is the area of the cross-section, and  $I(x)$  is the second moment of the area of the cross-section about the neutral axis.

It can be shown that for an infinitesimal element of the beam, the ratio of the rotational kinetic energy to the translational kinetic energy is approximately of the order of  $(h/l)^2$ , where  $h$  is the in-plane thickness of the beam. Since for a long and slender beam  $h \ll l$ , the rotational kinetic energy may be ignored [8,9]. Additionally, since in a planar beam flexure,  $u(x,t)$  is approximately two orders of magnitude smaller than  $w(x,t)$ , i.e.,  $u(x,t) = O(w(x,t)^2)$ , the axial kinetic energy of a beam element is at least four orders of magnitude smaller than its transverse kinetic energy, and therefore may also be ignored [8]. Thus, the total kinetic energy is simply given by

$$T = \frac{1}{2} \int_0^l \left( \frac{\partial w}{\partial t} \right)^2 \rho \cdot A \cdot dx + \frac{M}{2} \left( \left( \frac{\partial u(l,t)}{\partial t} \right)^2 + \left( \frac{\partial w(l,t)}{\partial t} \right)^2 \right) \quad (3)$$

where  $\rho$  is the material density and  $M$  is the tip mass.

Assuming that the beam vibrates in viscously damped media and assuming that the axial damping is negligible with respect to transverse damping, the virtual external work done on the beam by distributed damping loads would be

$$\delta W_e = - \int_0^l c_t \frac{\partial w(x,t)}{\partial x} \delta w(x,t) dx \quad (4)$$

where  $c_t$  is the damping coefficient per unit length in the transverse direction.

Now using the generalized Hamilton's principle, the equations governing the nonlinear dynamics of a beam undergoing large in-plane motions and the related geometric boundary conditions are obtained as follows:

$$\begin{aligned} \frac{\partial^2}{\partial x^2} \left( E \cdot I \frac{\partial^2 w}{\partial x^2} \right) - \frac{\partial}{\partial x} \left( E \cdot A(x) \left( \frac{\partial u}{\partial x} + \frac{1}{2} \left( \frac{\partial w}{\partial x} \right)^2 \right) \frac{\partial w}{\partial x} \right) \\ + c_t \frac{\partial w}{\partial t} + \frac{\partial}{\partial t} \left( \rho \cdot A(x) \cdot \frac{\partial w}{\partial t} \right) = - \frac{\partial}{\partial t} \left( M \frac{\partial w}{\partial t} \right) \hat{f}(l) \end{aligned} \quad (5)$$

$$\frac{d}{dt} \left( M \frac{du(l,t)}{dt} \right) + E \cdot A(x) \left( \frac{\partial u}{\partial x} + \frac{1}{2} \left( \frac{\partial w}{\partial x} \right)^2 \right) = 0 \quad (6)$$

$$u(0, t) = w(0, t) = \left. \frac{\partial w(x, t)}{\partial x} \right|_{x=0} = 0 \quad (7)$$

In Eq. (5),  $\hat{f}(x)$  is the Dirac delta function which is used to model the concentrated inertial load at  $x = l$ .

In long slender beams where  $u(x, t) = O(w(x, t)^2)$ , the axial inertia of the beam can be ignored compared with the concentrated inertial loads applied at the tip of the beam [8]. Assuming that axial damping is also negligible, the axial force  $E \cdot A(x) \cdot (\partial u / \partial x + 1/2(\partial w / \partial x)^2)$  would remain constant along the neutral axis of the beam. In such a condition, Eq. (5) is simplified as

$$\begin{aligned} \frac{\partial^2}{\partial x^2} \left( E \cdot I \frac{\partial^2 w}{\partial x^2} \right) - E \cdot A(x) \left( \frac{\partial u}{\partial x} + \frac{1}{2} \left( \frac{\partial w}{\partial x} \right)^2 \right) \frac{\partial^2 w}{\partial x^2} \\ + c_t \frac{\partial w}{\partial t} + \frac{\partial}{\partial t} \left( \rho \cdot A(x) \cdot \frac{\partial w}{\partial t} \right) = - \frac{\partial}{\partial t} \left( M \frac{\partial w}{\partial t} \right) \hat{f}(l) \end{aligned} \quad (8)$$

Additionally, since axial force  $E \cdot A(x) \cdot (\partial u / \partial x + 1/2(\partial w / \partial x)^2)$  is constant along the neutral axis of the beam, one can say

$$E \cdot A(x) \left( \frac{\partial u}{\partial x} + \frac{1}{2} \left( \frac{\partial w}{\partial x} \right)^2 \right) = \frac{1}{l} \int_0^l \left( E \cdot A(x) \left( \frac{\partial u}{\partial x} + \frac{1}{2} \left( \frac{\partial w}{\partial x} \right)^2 \right) \right) dx \quad (9)$$

Using integration by parts, Eq. (9) can be expressed as

$$\begin{aligned} E \cdot A(x) \left( \frac{\partial u}{\partial x} + \frac{1}{2} \left( \frac{\partial w}{\partial x} \right)^2 \right) = \frac{E \cdot A(l)}{l} \left( u(l, t) + \frac{1}{2} \int_0^l \left( \frac{\partial w}{\partial x} \right)^2 dx \right) \\ - \frac{1}{l} \int_0^l \frac{d(E \cdot A(x))}{dx} \left( u(x, t) + \frac{1}{2} \int_0^x \left( \frac{\partial w}{\partial x} \right)^2 dx \right) dx \end{aligned} \quad (10)$$

In this paper, it is assumed that the beam's cross-sectional geometry and material remains constant along the beam length. Therefore, with  $d(E \cdot A(x))/dx = 0$ , Eq. (10) can be further simplified as

$$E \cdot A(x) \left( \frac{\partial u}{\partial x} + \frac{1}{2} \left( \frac{\partial w}{\partial x} \right)^2 \right) = \frac{E \cdot A}{l} \left( u(l, t) + \frac{1}{2} \int_0^l \left( \frac{\partial w}{\partial x} \right)^2 dx \right) \quad (11)$$

With the assumption that the second moment of area of cross-section remains constant along the beam length and substituting Eq. (11) into Eqs. (8) and (6), the governing equations of the dynamic behavior of the flexure beam with tip mass can be obtained as

$$\begin{aligned} E \cdot I \frac{\partial^4 w}{\partial x^4} - \frac{E \cdot A}{l} \left( u(l, t) + \frac{1}{2} \int_0^l \left( \frac{\partial w}{\partial x} \right)^2 dx \right) \frac{\partial^2 w}{\partial x^2} + c_t \frac{\partial w}{\partial t} \\ + \frac{\partial}{\partial t} \left( \rho \cdot A \frac{\partial w}{\partial t} \right) = - \frac{\partial}{\partial t} \left( M \frac{\partial w}{\partial t} \right) \hat{f}(l) \end{aligned} \quad (12)$$

$$\frac{d}{dt} \left( M \frac{du(l, t)}{dt} \right) + \frac{E \cdot A}{l} \left( u(l, t) + \frac{1}{2} \int_0^l \left( \frac{\partial w}{\partial x} \right)^2 dx \right) = 0 \quad (13)$$

For convenience, the following dimensionless variables are introduced:

$$\hat{x} = \frac{x}{l}; \quad \hat{w} = \frac{w}{l}; \quad \hat{u} = \frac{u}{l}; \quad \hat{t} = t \sqrt{\frac{E \cdot I}{\rho \cdot A \cdot l^4}} \quad (14)$$

By substituting these dimensionless quantities into Eqs. (5) and (6), dropping the hats, and assuming  $\rho \cdot A$  and  $M$  are constant with respect to time, the following equations may be derived:

$$\begin{aligned} \frac{\partial^4 w}{\partial x^4} - \sigma_1 \left( u(t) + \frac{1}{2} \int_0^1 \left( \frac{\partial w}{\partial x} \right)^2 dx \right) \frac{\partial^2 w}{\partial x^2} + \frac{\partial^2 w}{\partial t^2} + C_t \frac{\partial w}{\partial t} \\ + \sigma_2 \frac{\partial^2 w(x, t)}{\partial t^2} \hat{f}(1) = 0 \end{aligned} \quad (15)$$

$$\lambda \frac{d^2 u(t)}{dt^2} + \left( u(t) + \frac{1}{2} \int_0^1 \left( \frac{\partial w}{\partial x} \right)^2 dx \right) = 0 \quad (16)$$

where  $u(t)$  is the normalized axial displacement of the tip mass and

$$\sigma_1 = \frac{Al^2}{I}; \quad \sigma_2 = \frac{M}{\rho \cdot A \cdot l} \quad (17)$$

$$\lambda = \frac{M}{\rho \cdot A \cdot lAl^2}; \quad C_t = \frac{c_t l^2}{\sqrt{\rho \cdot A \cdot E \cdot I}} \quad (18)$$

The first mode of a typical system is generally the most important one. When the system is excited by a broadband signal, most of the input excitation energy is injected into this first mode. Assuming this to be the case for the system being considered, one may employ the Galerkin projection method [8]. Accordingly, the transverse response of the system to an initial disturbance can be assumed to be as follows:

$$w(x, t) = \frac{\varphi(x)}{\varphi(1)} w(t) \quad (19)$$

Here,  $w(t)$  is the transverse displacement of the beam tip. Furthermore,  $\varphi(x)$  is the first linear undamped transversal vibrational mode of the system.  $\varphi(x)$  can be used as the basis function for describing the nonlinear behavior of the system. For a beam with a tip mass,  $\varphi(x)$  is given by [9]

$$\begin{aligned} \varphi(x) = \{ \cos(\beta x) - \cosh(\beta x) \} - \\ \frac{\cos(\beta) + \cosh(\beta)}{\sin(\beta) + \sinh(\beta)} \{ \sin(\beta x) - \sinh(\beta x) \} \end{aligned} \quad (20)$$

In this equation,  $\beta$  is the smallest positive root of Eq. (21)

$$1 + \frac{1}{\cos(\beta) \cosh(\beta)} - \frac{M}{m} \beta \{ \tan(\beta) - \tanh(\beta) \} = 0 \quad (21)$$

It needs to be noted that  $u(x, t)$  did not appear in the equations of motion (12) and (13). However, if the area of cross-section was assumed to be variable with respect to  $x$ , then the equations would contain both  $u(x, t)$  and  $w(x, t)$ . In such a case, in order to reduce the governing partial differential equations of motion to ordinary ones, an axial mode-shape would be needed along with a transverse mode-shape. In general, analytical functions are not available for the transverse and axial mode-shapes of beams with variable cross-section. Therefore, the proposed analytical approach in this paper is valid only for beam flexures with constant cross-section.

Substituting Eq. (19) into Eq. (15), multiplying it by  $\varphi(x)$  and then integrating the resulting equation over the dimensionless domain, the following nonlinear ordinary differential equation is obtained:

$$\begin{aligned} \frac{d^2 w(t)}{dt^2} + (c_2/c_1) \frac{dw(t)}{dt} + (c_3/c_1) w(t) \\ + (c_4/c_1) w(t)^3 + (c_5/c_1) w(t) u(t) = 0 \end{aligned} \quad (22)$$

Furthermore, by substituting Eq. (19) into Eq. (16), the following equation is obtained for the axial displacement of the beam tip:

$$\frac{d^2 u(t)}{dt^2} + (1/\lambda)u(t) + (d_1/\lambda)w(t)^2 = 0 \quad (23)$$

In Eqs. (22) and (23),  $c_i$  ( $i=1-5$ ) and  $d_1$  are defined as follows:

$$c_1 = \int_0^1 (\varphi(x)^2 + \sigma_2 \varphi(x)^2 \tilde{f}(1)) dx \quad (24)$$

$$c_2 = C_t \int_0^1 \varphi(x)^2 dx \quad (25)$$

$$c_3 = \int_0^1 \varphi(x) \frac{d^4 \varphi(x)}{dx^4} dx \quad (26)$$

$$c_4 = -\frac{\sigma_1}{2\varphi(1)^2} \int_0^1 \left(\frac{d\varphi(x)}{dx}\right)^2 dx \times \int_0^1 \varphi(x) \frac{d^2 \varphi(x)}{dx^2} dx \quad (27)$$

$$c_5 = -\sigma_1 \int_0^1 \varphi(x) \frac{d^2 \varphi(x)}{dx^2} dx \quad (28)$$

$$d_1 = \frac{1}{2\varphi(1)^2} \int_0^1 \left(\frac{d\varphi(x)}{dx}\right)^2 dx \quad (29)$$

In order for the coefficients of equations (22) and (23) to appear at the same order, the following dimensionless variable is introduced:

$$\tau = t/\sqrt{\lambda} \quad (30)$$

Substituting Eq. (30) into Eqs. (22) and (23), the following equations are obtained:

$$\frac{d^2 w(\tau)}{d\tau^2} + \omega_n^2 \cdot w(\tau) + C_1 \frac{dw(\tau)}{d\tau} + C_2 w(\tau)^3 + C_3 w(\tau)u(\tau) = 0 \quad (31)$$

$$\frac{d^2 u(\tau)}{d\tau^2} + u(\tau) + d_1 w(\tau)^2 = 0 \quad (32)$$

where  $\omega_n$  and  $C_i$ 's ( $i=1-3$ ) are defined as

$$\omega_n = \sqrt{\frac{c_3 \lambda}{c_1}}; \quad C_1 = \frac{c_2}{c_1} \sqrt{\lambda}; \quad C_2 = \frac{c_4 \lambda}{c_1}; \quad C_3 = \frac{c_5 \lambda}{c_1} \quad (33)$$

It should be noted that the natural frequency  $\omega_n$  in Eq. (31) is not the actual frequency but instead a normalized one. Also, in Eq. (32), which captures axial dynamics, the first term corresponds to elastic stretching and the third term corresponds to geometric nonlinearity. If elastic stretching had not been included in the formulation, then this equation would simply reduce to a kinematic relation between the transverse and axial displacements.

### 3 Solution Procedure

While Eqs. (31) and (32) may be solved numerically using a finite difference method (as done later in Sec. 4 for the purpose of validation), that approach does not offer any design insight. Instead, the multiple time scales perturbation method is used here to derive analytical closed-form solutions to these equations. In this method, time variable  $\tau$  is expanded in terms of multiple time scales  $T_0 = \tau$  and  $T_1 = \varepsilon\tau$  where  $\varepsilon$  is a small book-keeping parameter [8]. Using the chain rule, the first and the second derivatives with respect to  $\tau$  become

$$\frac{d}{d\tau}(\cdot) = \frac{\partial}{\partial T_0}(\cdot) + \varepsilon \frac{\partial}{\partial T_1}(\cdot) \quad (34)$$

$$\frac{d^2}{d\tau^2}(\cdot) = \frac{\partial^2}{\partial T_0^2}(\cdot) + 2\varepsilon \frac{\partial^2}{\partial T_0 \partial T_1}(\cdot) + \varepsilon^2 \frac{\partial^2}{\partial T_1^2}(\cdot) \quad (35)$$

**3.1 The Nonresonant Case.** Although the transverse displacement of the beam's tip is much larger than the beam's thickness, resulting in the geometric nonlinearities seen in Eqs. (31) and (32), it can still be assumed to be an order of magnitude smaller than the beam's length for most applications of interest. This implies

$$w(\tau) \sim O(\varepsilon) \quad (36)$$

Considering Eq. (32) and recognizing that  $d_1 \sim O(1)$  (see Table 2 for typical numbers), it can be argued that at least in the static case where  $d^2 u(\tau)/d\tau^2 = 0$

$$u(\tau) \sim O(\varepsilon^2) \quad (37)$$

These results, which also agree with a physical understanding of the beam mechanics, have been shown to be valid in previous analytical results [17].

Therefore, the solution of Eqs. (31) and (32) are sought in the form

$$u(T_0, T_1) = \varepsilon^2 (u_0(T_0, T_1) + \varepsilon u_1(T_0, T_1) + \dots) \quad (38)$$

$$w(T_0, T_1) = \varepsilon (w_0(T_0, T_1) + \varepsilon w_1(T_0, T_1) + \dots) \quad (39)$$

Assuming that the damping coefficient, i.e.,  $C_1$ , is small, one may state

$$C_1 = \varepsilon C_{10} \quad (40)$$

By substituting Eqs. (34), (35), (38), (39), and (40) into Eqs. (31) and (32), and equating the coefficients of like powers of  $\varepsilon$  in both sides of each equation, the following sets of equations are obtained:

$$\varepsilon^1: \frac{\partial^2 w_0(T_0, T_1)}{\partial T_0^2} + \omega_n^2 w_0(T_0, T_1) = 0 \quad (41)$$

$$\varepsilon^2: \frac{\partial^2 u_0(T_0, T_1)}{\partial T_0^2} + u_0(T_0, T_1) = -d_1 w_0(T_0, T_1)^2 \quad (42)$$

$$\varepsilon^2: \frac{\partial^2 w_1(T_0, T_1)}{\partial T_0^2} + \omega_n^2 w_1(T_0, T_1) = -2 \frac{\partial^2 w_0(T_0, T_1)}{\partial T_1 \partial T_0} - C_{10} \frac{\partial w_0(T_0, T_1)}{\partial T_0} \quad (43)$$

$$\varepsilon^3: \frac{\partial^2 u_1(T_0, T_1)}{\partial T_0^2} + u_1(T_0, T_1) = -2 \frac{\partial^2 u_0(T_0, T_1)}{\partial T_0 \partial T_1} - 2d_1 w_0(T_0, T_1)w_1(T_0, T_1) \quad (44)$$

Equations (41) and (42) constitute a system of linear ordinary differential equations with constant coefficients and their solution can be written as

$$w_0(T_0, T_1) = A(T_1) \exp(i\omega_n T_0) + cc \quad (45)$$

$$u_0(T_0, T_1) = \frac{d_1 A(T_1)^2}{-1 + 4\omega_n^2} \exp(2i\omega_n T_0) - d_1 A(T_1)\bar{A}(T_1) + B(T_1) \exp(iT_0) + cc \quad (46)$$

where  $\bar{A}(T_1)$  and  $\bar{B}(T_1)$  are complex conjugate of  $A(T_1)$  and  $B(T_1)$ , respectively. In these equations, as well as in the rest of this paper,  $cc$  means the complex conjugate of all of the preceding terms.

Substituting Eqs. (45) and (46) into Eq. (43), the latter can be readily solved using linear ordinary differential equation solution techniques. But any particular solution of this equation would contain a secular term,  $T_0 \exp(\pm i\omega_n T_0)$ , unless the coefficient of



$\exp(I\omega_n T_0)$  in the right-hand side of Eq. (43) is zero. Therefore, the following condition has to be satisfied in order to avoid any secular terms in the response:

$$2I\omega_n \frac{dA(T_1)}{dT_1} + I\omega_n C_{10} A(T_1) = 0 \quad (47)$$

To solve Eq. (47), it is convenient to write  $A(T_1)$  in the polar form

$$A(T_1) = \frac{1}{2} a_1(T_1) \exp(\alpha_1(T_1)I) \quad (48)$$

By substituting Eq. (48) into Eq. (47) along with making the necessary simplifications, and equating both the real and imaginary parts of these equations with zero, the following conditions are obtained:

$$\frac{da_1(T_1)}{dT_1} + \frac{1}{2} C_{10} a_1(T_1) = 0 \quad (49)$$

$$\frac{d\alpha_1(T_1)}{dT_1} = 0 \quad (50)$$

The solution of Eqs. (49) and (50) is simply

$$a_1(T_1) = a_1 \exp\left(-\frac{1}{2} C_{10} T_1\right) \quad (51)$$

$$\alpha_1(T_1) = \alpha_1 \quad (52)$$

Using Eqs. (45), (48), (51), and (52),  $w_0(T_0, T_1)$  is obtained as follows:

$$w_0(T_0, T_1) = a_1 \exp\left(-\frac{1}{2} C_{10} T_1\right) \cos(\omega_n T_0 + \alpha_1) \quad (53)$$

By substituting Eq. (53) in Eq. (43), the particular solution of the resulting equation is easily obtained as

$$w_1(T_0, T_1) = 0 \quad (54)$$

Using Eqs. (46), (53), and (54), Eq. (44) may be rewritten in the form

$$\frac{\partial^2 u_1(T_0, T_1)}{\partial T_0^2} + u_1(T_0, T_1) = 2I \frac{dB(T_1)}{dT_1} \exp(IT_0) + \frac{I \cdot d_2 \alpha_0^2 \omega_n C_{10} \exp(-C_{10} T_1)}{1 - 4\omega_n^2} \exp(2I(\alpha_0 + \omega_n T_0)) + cc \quad (55)$$

Appearance of secular terms in the response of Eq. (55) can be avoided by using a similar procedure as above. Doing so, one can obtain

$$2I \frac{dB(T_1)}{dT_1} = 0 \quad (56)$$

To solve Eq. (56), it is convenient to write  $B(T_1)$  in the polar form

$$B(T_1) = \frac{1}{2} b(T_1) \exp(I\beta(T_1)) \quad (57)$$

By substituting Eq. (57) in Eq. (56), and separating real and imaginary parts of the obtained algebraic expressions, the following conditions are obtained:

$$-b(T_1) \frac{d\beta(T_1)}{dT_1} = 0 \quad (58)$$

$$\frac{db(T_1)}{dT_1} = 0 \quad (59)$$

The solutions of Eqs. (58) and (59) are

$$\beta(T_1) = \beta_0 \quad (60)$$

$$b(T_1) = b_0 \quad (61)$$

Therefore, using Eqs. (46), (57), (60), and (61),  $u_0(T_0, T_1)$  is obtained as

$$u_0(T_0, T_1) = b_0 \cos(T_0 + \beta_0) - \frac{1}{2} d_1 a_1^2 \exp(-C_{10} T_1) \times \left(1 + \frac{\cos(2(\omega_n T_0 + \alpha_0))}{1 - 4\omega_n^2}\right) \quad (62)$$

By substituting  $T_0 = \tau$  and  $T_1 = \varepsilon\tau$ , in Eqs. (53) and (62), a zero-order approximate solution for  $w(\tau)$  and  $u(\tau)$  is obtained as

$$w(\tau) = \varepsilon a_1 \exp\left(-\frac{1}{2} C_{10} \varepsilon\tau\right) \cos(\omega_n \tau + \alpha_0) \quad (63)$$

$$u(\tau) = \varepsilon^2 b_0 \cos(\tau + \beta_0) - \frac{1}{2} d_1 (\varepsilon a_1)^2 \exp(-C_{10} \varepsilon\tau) \left(1 + \frac{\cos(2(\omega_n \tau + \alpha_0))}{1 - 4\omega_n^2}\right) \quad (64)$$

Since  $\varepsilon$  is a book-keeping dummy parameter, one can substitute  $a = \varepsilon a_1$  and  $b_1 = \varepsilon^2 b_0$  and using Eq. (40), the zero order perturbation approximation for  $w(\tau)$  and  $u(\tau)$  can be further simplified as

$$w(\tau) = a \exp\left(-\frac{1}{2} C_{10} \tau\right) \cos(\omega_n \tau + \alpha_0) \quad (65)$$

$$u(\tau) = b_1 \cos(\tau + \beta_0) - \frac{1}{2} d_1 a^2 \exp(-C_{10} \tau) \times \left(1 + \frac{\cos(2(\omega_n \tau + \alpha_0))}{1 - 4\omega_n^2}\right) \quad (66)$$

In above solution for  $u(\tau)$ , the first term corresponds to axial stretching of the beam, while the second term corresponds to the geometric nonlinearity associated with arc-length conservation.

**3.2 The Resonant Case.** Next, one may mathematically analyze the resonant case where  $\omega_n$  is close to  $1/2$ , which represents a condition of internal resonance in the system of nonlinear ordinary differential equations given by Eqs. (31) and (32). It is important to note that this normalized value of  $\omega_n = 1/2$  actually corresponds to a large frequency. For the example case considered in Sec. 4 below, this natural frequency corresponds to 5874 rad/s. At such large frequencies, the approximations made in deriving Eqs. (31) and (32) break down. To accurately analyze the dynamics of the system in this frequency range, several transverse and axial modes will need to be considered and the axial kinetic energy cannot be ignored. Therefore, solving the above equations for the case when  $\omega_n \approx 1/2$  is a strictly mathematical exercise and of little physical relevance. Nevertheless, an analytical solution is presented here for the sake of completeness.

Equation (66) shows that when  $\omega_n \approx 1/2$ ,  $u(\tau)$  increases significantly which is a sign of resonance. Therefore, to solve near this resonance state, one needs to start perturbation expansion of  $u(\tau)$  from a lower order, i.e., from  $\varepsilon$  instead of  $\varepsilon^2$

$$u(T_0, T_1) = \varepsilon(u_0(T_0, T_1) + \varepsilon u_1(T_0, T_1) + \dots) \quad (67)$$

In this case, by following a similar procedure presented for the nonresonant case, the following equations are obtained for  $u_i(T_0, T_1)$  and  $w_i(T_0, T_1)$ , where  $i = 0, 1$ :

$$\varepsilon^1: \frac{\partial^2 w_0(T_0, T_1)}{\partial T_0^2} + \omega_n^2 w_0(T_0, T_1) = 0 \quad (68)$$

$$\varepsilon^1: \frac{\partial^2 u_0(T_0, T_1)}{\partial T_0^2} + u_0(T_0, T_1) = 0 \quad (69)$$

$$\varepsilon^2: \frac{\partial^2 w_1(T_0, T_1)}{\partial T_0^2} + \omega_n^2 w_1(T_0, T_1) = -2 \frac{\partial^2 w_0(T_0, T_1)}{\partial T_1 \partial T_0} - C_{10} \frac{\partial w_0(T_0, T_1)}{\partial T_0} - C_3 w_0(T_0, T_1) u_0(T_0, T_1) \quad (70)$$

$$\varepsilon^2: \frac{\partial^2 u_1(T_0, T_1)}{\partial T_0^2} + u_1(T_0, T_1) = -2 \frac{\partial^2 u_0(T_0, T_1)}{\partial T_1 \partial T_0} - d_1 w_0(T_0, T_1)^2 \quad (71)$$

The solution of Eq. (68) is of the same form as given in Eq. (45) and the solution of Eq. (69) is as

$$u_0(T_0, T_1) = B(T_1) \exp(IT_0) + cc \quad (72)$$

In the internal resonance state, the nearness of  $\omega_n$  can be described mathematically as

$$\omega_n = \frac{1}{2} + \varepsilon\sigma \quad (73)$$

where  $\sigma \sim O(1)$ .

Using Eq. (73), one can conclude

$$\exp(\pm I\omega_n T_0) = \exp\left(\pm \frac{IT_0}{2}\right) \exp(\pm I\sigma T_1) \quad (74)$$

$$\exp(\pm IT_0) = \exp(\pm 2I\omega_n T_0) \exp(\mp 2I\sigma T_1) \quad (75)$$

By substituting Eqs. (45), (72), (74), and (75) in the right-hand side of Eqs. (70) and (71), the terms capable of producing secular terms in the response of these latter equations are obtained as

$$2I\omega_n \frac{dA(T_1)}{dT_1} + IC_{10}\omega_n A(T_1) = 0 \quad (76)$$

$$2I \frac{dB(T_1)}{dT_1} + d_1 A(T_1)^2 \exp(2I\sigma T_1) = 0 \quad (77)$$

Substituting Eqs. (48) and (57) into Eqs. (76) and (77), and equating the real and imaginary parts to zero gives

$$\omega_n \frac{da_1(T_1)}{dT_1} + \frac{1}{2} \omega_n C_1 a_1(T_1) = 0 \quad (78)$$

$$\frac{d\alpha_1(T_1)}{dT_1} = 0 \quad (79)$$

$$\frac{db(T_1)}{dT_1} + \frac{1}{4} d_1 a_1(T_1)^2 \sin(2\alpha_1(T_1) - \beta(T_1) + 2\sigma T_1) = 0 \quad (80)$$

$$-b(T_1) \frac{d\beta(T_1)}{dT_1} + \frac{1}{4} d_1 a_1(T_1)^2 \cos(2\alpha_1(T_1) - \beta(T_1) + 2\sigma T_1) = 0 \quad (81)$$

Equations (78)–(81) can be transformed into an autonomous system by letting

$$\gamma(T_1) = 2\alpha_1(T_1) - \beta(T_1) + 2\sigma T_1 \quad (82)$$

The results are

$$\frac{da_1(T_1)}{dT_1} = -\frac{1}{2} C_{10} a_1(T_1) \quad (83)$$

**Table 1 Characteristics of the simulated beam and its tip mass**

Symbol	Definition	Value
$E$	Young's Modulus of elasticity of the beam material	69 GPa
$\rho$	Density of the beam material	7800 kg/m <sup>3</sup>
$l$	Beam's length	0.15 m
$b$	Beam's width	0.015 m
$h$	Beam's thickness	0.001 m
$M$	Tip mass	0.050 kg

**Table 2 Values of the intermediate parameters defined in the analysis. Parameters listed without any units represent normalized quantities.**

$A = 1.5 \times 10^{-5} \text{ m}^2$	$c_1 = 13.033$
$I = 1.25 \times 10^{-12} \text{ m}^4$	$c_3 = 13.729$
$m = 1.755 \times 10^{-2} \text{ kg}$	$c_4 = 8.845 \times 10^5$
$\sigma_1 = 2.7 \times 10^5$	$c_5 = 1.477 \times 10^6$
$\sigma_2 = 2.849$	$d_1 = 0.598$
$\lambda_1 = 1.055 \times 10^{-5}$	$\omega_n = 3.334 \times 10^{-3}$
$\beta = 0.993$	$C_2 = 0.716$
$C_1 = 0.001$	$C_3 = 1.196$

$$\frac{d\gamma(T_1)}{dT_1} = 2\sigma - \frac{d\beta(T_1)}{dT_1} \quad (84)$$

$$\frac{db(T_1)}{dT_1} = -\frac{1}{4} d_1 a_1(T_1)^2 \sin(\gamma(T_1)) \quad (85)$$

$$b(T_1) \frac{d\beta(T_1)}{dT_1} = \frac{1}{4} d_1 a_1(T_1)^2 \cos(\gamma(T_1)) \quad (86)$$

By solving Eqs. (83)–(86), one can find  $a_1(T_1)$ ,  $\gamma(T_1)$ ,  $b(T_1)$ , and  $\beta(T_1)$ .

After eliminating secular terms, the solution of Eq. (71) becomes

$$u_1(T_0, T_1) = -\frac{1}{2} d_1 a_1(T_1)^2 \quad (87)$$

Substituting Eq. (48) in the response of Eq. (68) (i.e., Eq. (45)), a zero order approximation for  $w(\tau)$  is obtained as

$$w(\tau) = a \exp\left(-\frac{1}{2} C_1 \tau_1\right) \cos(\omega_n T_0 + \alpha_1) \quad (88)$$

where  $a = \varepsilon a_1$ .

Similarly by substituting Eqs. (87) and (72) in Eq. (67), a first-order approximation for  $u(\tau)$  is obtained as

$$u(\tau) = -\frac{1}{2} d_1 a^2 \exp(-C_1 \tau) + b_1(\tau) \cos(\tau + \beta(\tau)) \quad (89)$$

where  $b_1(\tau) = \varepsilon^2 b(\tau)$

## 4 Case Study

A flexure beam with a tip mass with material and geometric properties listed in Table 1 is considered.

To provide a sense of the order of magnitude of the intermediate parameters defined in the above derivations, their values are compiled in Table 2.

In addition, the damping coefficient  $c_t$  is selected such that the final damping coefficient becomes  $C_1 = 0.001$ , a nominal small value. For a practical choice of dimensions, as listed in Table 1, even though the non-normalized natural frequency is finite (equal to 37.6 rad/s), the normalized natural frequency  $\omega_n$  in Eq. (31) is very small. This is simply a consequence of the fact that time is

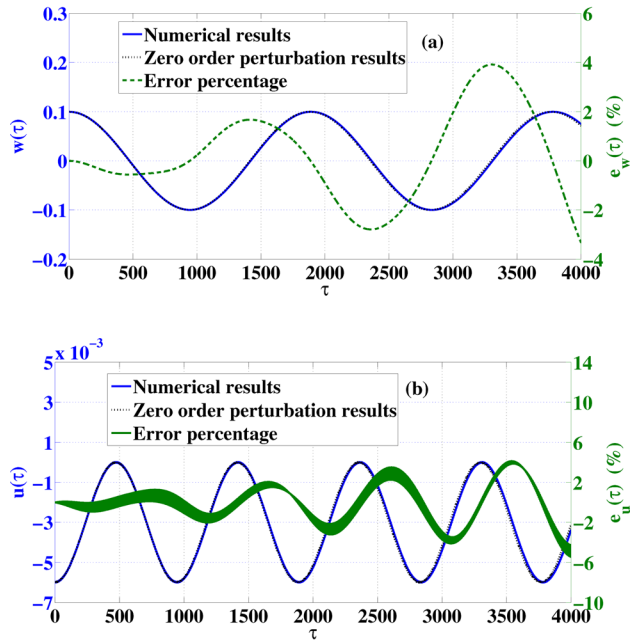


**Fig. 3** Comparison of analytical results with numerical simulations for an undamped system with initial conditions  $w(0) = 0.1$  and  $u(0) = -0.006$ . (a) Tip transverse displacement and (b) tip axial displacement.

normalized via Eq. (30) using the natural frequency of the axial direction dynamics, given by Eq. (23).

Figures 3 and 4 present the results of the above analytical model validated against numerical simulations for the undamped and damped cases, respectively, for a set of initial conditions. In these figures, the numerical results have been obtained by solving Eqs. (31) and (32) using the ode45 initial value solver in MATLAB [18]. The error percentages  $e_w(\tau)$  and  $e_u(\tau)$ , plotted on the right side vertical axes of these figures, are defined as follows:

$$e_w(\tau) = \left[ \frac{w_{\text{Analytic}}(\tau) - w_{\text{Numeric}}(\tau)}{w_{\text{Numeric}}(0)} \right] \times 100\% \quad (90)$$

$$e_u(\tau) = \left[ \frac{u_{\text{Analytic}}(\tau) - u_{\text{Numeric}}(\tau)}{u_{\text{Numeric}}(0)} \right] \times 100\% \quad (91)$$

where  $w_{\text{Analytic}}(\tau)$  and  $u_{\text{Analytic}}(\tau)$  are the analytical transverse and axial response, respectively, and  $w_{\text{Numeric}}(\tau)$  and  $u_{\text{Numeric}}(\tau)$  are the numerical transverse and axial response, respectively.

It is observed that when there is no internal resonance in the system, the analytical results follow the numerical ones, thus validating the accuracy of the analytical modeling presented in this paper.

The normalized transverse dynamics presented in Figs. 3(a) and 4(a) consists of a large-amplitude low-frequency component. The normalized axial dynamic presented in Figs. 3(b) and 4(b) is composed of a high-frequency small-amplitude component and a low-frequency large-amplitude component. The former is due to the effect of the transverse vibration of the beam on its axial vibration (i.e., geometric nonlinearity of arc-length conservation), while the latter is the direct consequence of the large axial stiffness associated with the elastic stretching of the beam. Zoomed views of the latter component are shown in Fig. 5. This component would not appear if the analytical formulation did not include elastic stretching.

Although the amplitudes of response in the analytical and numerical results are very close, there exist small discrepancies in the frequencies. These discrepancies lead to the errors seen in Figs. 3 and 4, and the phase mismatch in Fig. 5. For the particular

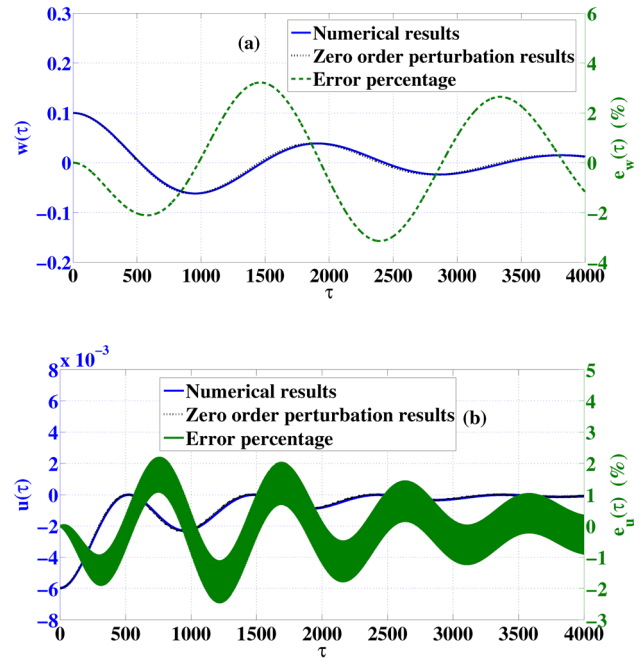


**Fig. 4** Comparison of the analytical results with numerical simulations for a damped system with  $C_1 = 0.001$  and initial conditions  $w(0) = 0.1$  and  $u(0) = -0.006$ . (a) Tip transverse displacement and (b) tip axial displacement.

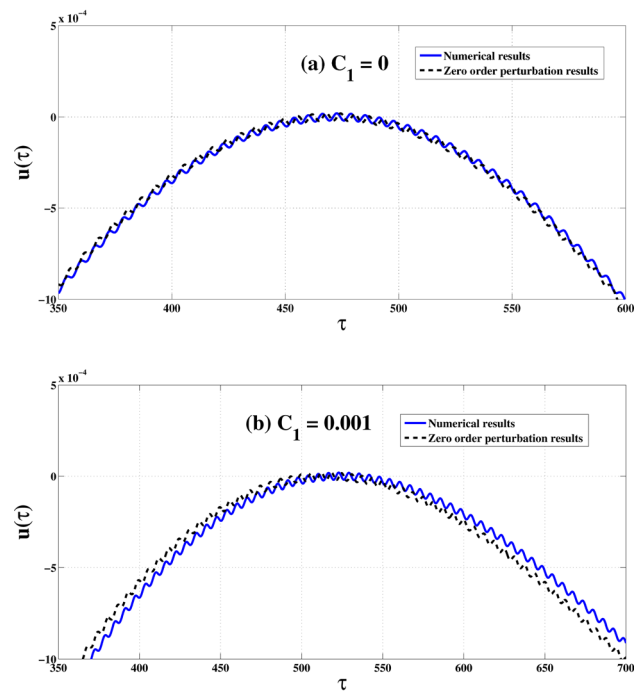


**Fig. 5** Zoomed view of the normalized axial displacement: (a) undamped system, and (b) damped system,  $C_1 = 0.001$

case considered here, the frequency discrepancy between low-frequency components is less than 0.36% for the undamped case and less than 1.35% for the damped case. The frequency discrepancy between the high-frequency components is less than 0.3% for the undamped as well as damped case. Even though these discrepancies are small, over time they result in a phase mismatch as seen in Fig. 5, and an overall error as seen in Figs. 3 and 4. For the undamped case, this error grows to a maximum value when

the phase mismatch becomes 180 deg. However, in the damped case, which better represents a real situation, the error percentage decays with normalized time in spite of the phase mismatch because the amplitude itself decreases due to damping.

## 5 Results and Discussion

The importance of studying the dynamics of flexure mechanisms to better inform their design and optimization is well-recognized. However, the presence of effects, such as elastic stretching and geometric nonlinearities in flexure mechanics, can make this investigation complicated and nontrivial. From a design stand-point, several important questions arise: When should such effects be taken into consideration if designing for dynamic performance? What design changes can be made to mitigate or accentuate these effects? Therefore, as a starting point in a broader investigation, we modeled a simple beam flexure with a tip mass in this paper and analyzed its large-amplitude in-plane oscillations. Axial stretching of the beam and geometric nonlinearity associated with arc-length conservation were included. Once the equations of motion were formulated, analytical zero order and first order expressions for the beam tip displacement were derived and validated using numerical simulations.

The value of analytical results, such as (65) and (66), which provide closed-form free vibration solution for the nonresonant case ( $\omega_n \ll 1/2$ ), lies in the fact that they help identify when the axial stretching and geometric nonlinearity become important. For a given initial conditions,  $w(0)$  and  $u(0)$ , one can further show that the amplitude of transverse vibration,  $a$ , in expression (65) is of the order of  $w(0)$ . The axial vibration given by expression (66) has two components: a high-frequency (normalized value of 1) component with amplitude  $b_1$  which arises due to axial stretching, and a low-frequency (normalized value of  $\omega_n$ ) component with amplitude  $d_1 a^2 / 2(1 - 4\omega_n^2)$  which arises due to geometric nonlinearity. Moreover, the former amplitude can be shown to be approximately  $2d_1 \omega_n^2 w(0)^2 + (u(0) + d_1 w(0)^2)$ , while the latter amplitude is approximately  $d_1 w(0)^2 / 2$ .

Thus, closed-form analysis explicitly separates out the various physical effects in parametric mathematical terms. This helps elucidate how the physical parameters of the beam flexure (dimensions, material, tip mass, etc.) and initial conditions contribute to the various mathematical terms and associated physical effects that appear in the dynamics. For example, under certain conditions, the high-frequency component of the axial vibration associated with elastic stretching can become negligible compared with the low-frequency component associated with geometric nonlinearity, and vice versa. With this clear understanding, one can now make informed decisions regarding the choice of physical parameters, which is an essential aspect of design. This connection

between physical parameters, mathematical terms, and associated physical phenomena helps generate design insight.

As noted earlier, this work is still preliminary. Having investigated free vibrations here, the immediate next goal is to extend this analysis to forced vibrations, which are relevant in many applications. Furthermore, while the approximations and assumptions made in the analysis approach presented here are justified by physical and mathematical arguments, the final results are yet to be validated via experimental measurements. In addition to experimental validation, our on-going research effort includes extending the above analysis approach to include greater number of mode shapes in a single beam with tip mass, and to more complex flexure modules and mechanisms.

## References

- [1] Howell, L. L., 2001, *Compliant Mechanisms*, Wiley, New York.
- [2] Smith, S. T., 2000, *Flexures: Elements of Elastic Mechanisms*, Gordon & Breach, Amsterdam, Netherlands.
- [3] Awtar, S., Slocum, A., and Sevincer, E., 2007, "Characteristics of Beam-Based Flexure Modules," *ASME J. Mech. Des.*, **129**(6), pp. 625–639.
- [4] Su, W., and Cesnik, C. E. S., 2011, "Strain-Based Geometrically Nonlinear Beam Formulation for Modeling Very Flexible Aircraft," *Int. J. Solids Struct.*, **48**, pp. 2349–2360.
- [5] Awtar, S., 2004, "Synthesis and Analysis of Parallel Kinematic XY Flexure Mechanisms," Sc.D., Department of Mechanical Engineering, Massachusetts Institute of Technology, Cambridge, MA.
- [6] Awtar, S., and Parmar, G., 2013, "Design of a Large Range XY Nanopositioning System," *ASME J. Mech. Rob.*, **5**(2), p. 021008.
- [7] Fowler, A. G., Laskovski, A. N., Hammond, A. C., and Moheimani, S. O. R., 2012, "A 2-DOF Electrostatically Actuated MEMS Nanopositioner for On-Chip AFM," *J. Microelectromech. Syst.*, **21**, pp. 771–773.
- [8] Nayfeh, A. H., and Mook, D. T., 1979, *Nonlinear Oscillations*, Wiley, New York.
- [9] Rao, S. S., 2007, *Vibration of Continuous Systems*, Wiley, Hoboken, NJ.
- [10] Crespo Da Silva, M. R. M., 1988, "Non-Linear Flexural-Flexural-Torsional-Extensional Dynamics of Beams-I. Formulation," *Int. J. Solids Struct.*, **24**, pp. 1225–1234.
- [11] Crespo Da Silva, M. R. M., 1998, "A Reduced-Order Analytical Model for the Nonlinear Dynamics of a Class of Flexible Multi-Beam Structures," *Int. J. Solids Struct.*, **35**, pp. 3299–3315.
- [12] Nayfeh, A. H., 1973, "Nonlinear Transverse Vibrations of Beams With Properties That Vary Along the Length," *J. Acoust. Soc. Am.*, **53**, pp. 766–770.
- [13] Zaretsky, C. L., and Crespo da Silva, M. R. M., 1994, "Experimental Investigation of Non-Linear Modal Coupling in the Response of Cantilever Beams," *J. Sound Vib.*, **174**, pp. 145–167.
- [14] Hijmissen, J. W., and van Horsen, W. T., 2008, "On the Weakly Damped Vibrations of a Vertical Beam With a Tip-Mass," *J. Sound Vib.*, **310**, pp. 740–754.
- [15] Zavodney, L. D., and Nayfeh, A. H., 1989, "The Non-Linear Response of a Slender Beam Carrying a Lumped Mass to a Principal Parametric Excitation: Theory and Experiment," *Int. J. Non-Linear Mech.*, **24**, pp. 105–125.
- [16] Yu, Y. Q., Howell, L. L., Lusk, C., Yue, Y., and He, M. G., 2005, "Dynamic Modeling of Compliant Mechanisms Based on the Pseudo-Rigid-Body Model," *ASME J. Mech. Des.*, **127**(4), pp. 760–765.
- [17] Awtar, S., and Sen, S., 2010, "A Generalized Constraint Model for Two-Dimensional Beam Flexures: Nonlinear Strain Energy Formulation," *ASME J. Mech. Des.*, **132**(8), p. 081009.
- [18] MATLAB Product Help, R2010a, ode45 command.